

UVIT/AstroSat Investigation of a low luminous Blue Straggler Star in NGC 362: Detection of extremely low mass white dwarf as companion

Arvind K. DATTATREY^{1,2,*}, R. K. S. YADAV^{2,*}, Annapurni SUBRAMANIAM³
and Ravi S. SINGH²

¹ Aryabhata Research Institute of Observational Sciences, Manora Peak Nainital, 263001, India.

² Deen Dayal Upadhyay Gorakhpur University, Gorakhpur, Uttar Pradesh 273009, India.

³ Indian Institute of Astrophysics, Koramangala, Bangalore 560034, India.

* Corresponding authors: arvind@aries.res.in, rkant@aries.res.in

Abstract

In the present study, we identified an extremely low-mass white dwarf as a companion to a low luminous blue straggler star within the Galactic globular cluster NGC 362. To conduct the analysis, we utilized data obtained from various sources, including AstroSat's Ultra Violet Imaging Telescope, UVOT, and the 2.2-m ESO telescope. By examining the spectral energy distribution of the blue straggler star candidate, we successfully identified an extremely low-mass white dwarf as its binary companion. We determined the effective temperature, radius, and luminosity for both, the extremely low-mass white dwarf and the blue straggler star candidate. Specifically, the extremely low-mass white dwarf exhibits an effective temperature of 15000 K, a radius of $0.17 R_{\odot}$, a luminosity of $1.40 L_{\odot}$, and a mass range of $0.19-0.20 M_{\odot}$. Furthermore, the position of the straggler star within the cluster suggests their formation via the Case A/B mass-transfer mechanism in a low-density environment.

Keywords: Stars: blue straggler; Hertzsprung-Russell and CM diagrams; Globular star clusters: individual: NGC362

1. INTRODUCTION

Globular clusters (GCs) were among the earliest known celestial systems in which stars regularly interacted gravitationally. These interactions result in diverse phenomena, including two-body relaxation, mass segregation from core collapse, energy equipartition, stellar collisions, mass transfer, and binary star mergers. Gravitationally interacting binary stars can endure this process, in which the more massive star consumes its companion, growing in size and luminosity until it transforms into a blue straggler star (BSS).

Extensive research has been conducted on white dwarfs (WDs), which possess helium cores and are commonly referred to as extremely low-mass white dwarfs (ELM WDs). These unique

WDs have masses up to approximately $0.20 M_{\odot}$. It is believed that white dwarfs resulting from the evolution of isolated stars have a maximum mass of around $0.4 M_{\odot}$ which is connected to the age of the universe (Brown et al., 2010). Compact binary systems have been observed to contain white dwarfs with masses ranging from 0.1 to $0.4 M_{\odot}$ (Benvenuto and De Vito, 2004; Brown et al., 2010). These white dwarfs are thought to have formed due to mass loss in these binary systems.

The GC NGC 362 is located at the celestial coordinates (RA = $01^h 03^m 14.26^s$ and Dec = $-70^{\circ} 50' 55''.6$) in the constellation Tucana, situated in the Southern hemisphere. Estimates suggest that this cluster has an age of approximately 11 Gyr (Vasiliev and Baumgardt, 2021) and is located at a distance of 8.83 kpc from Earth. It exhibits a reddening value of ~ 0.05 mag and a metallicity [Fe/H] of ~ -1.3 dex (Harris, 2010).

2. DATA SETS AND THEIR REDUCTION

The GC NGC 362 is analyzed using images captured by the UVIT (Tandon et al. (2017)) instrument on the AstroSat satellite. The observations took place on November 11, 2016, using four UV bands: F148W, F169M, N245M, and N263M. In addition to the UVIT data, we used Ultraviolet Optical Telescope (UVOT) data. The raw data from the UVOT, sourced from the HEASARC archive, were processed using the HEA-Soft pipeline (Poole et al., 2008). The detailed information about the UVOT instrument and the photometric correction can be found in Poole et al. (2008). Furthermore, we included optical data from past observations conducted with the Wide-Field Imager (WFI) in U, B, V, R, and I bands mounted on the 2.2 m ESO/MPI Telescope. Detailed information about data and photometry has also been given in Dattatrey et al. (2023).

3. UV AND OPTICAL COLOR-MAGNITUDE DIAGRAMS

We conducted the present analysis by cross-matching the UVIT data with the Gaia EDR3 photometric data within a matching radius of $1''.5$. The membership probability of the stars is more than 80%, taken from Sahu et al. (2022). The membership probability has been determined using GAIA DR3 proper motions data. It is based on the comparison of the cluster-like stars' kinematics distribution and the field distribution. We created the UV-optical color-magnitude diagrams (CMDs) by considering the optical counterparts of UVIT detected sources.

To select the BSSs, we adopted the method given in Dattatrey et al. (2023). Basically, we made a box around the BSS sequence using CMD. To determine the bottom limit of the box, we computed the average magnitudes and colors with standard deviation (σ) of stars within one magnitude box near the main sequence (MS) turn-off point. The lower limit of the box is greater than 5σ from the MS turn-off. Our primary focus was on the FUV optical CMD (F148W, (F148W – G)), which provided crucial information about the cluster stars. In Figure 1 (left panel), we plotted the CMD, where blue symbols represent the BSSs. To interpret the CMD, we introduced dotted and solid lines representing the Zero-Age Main Sequence (ZAMS)

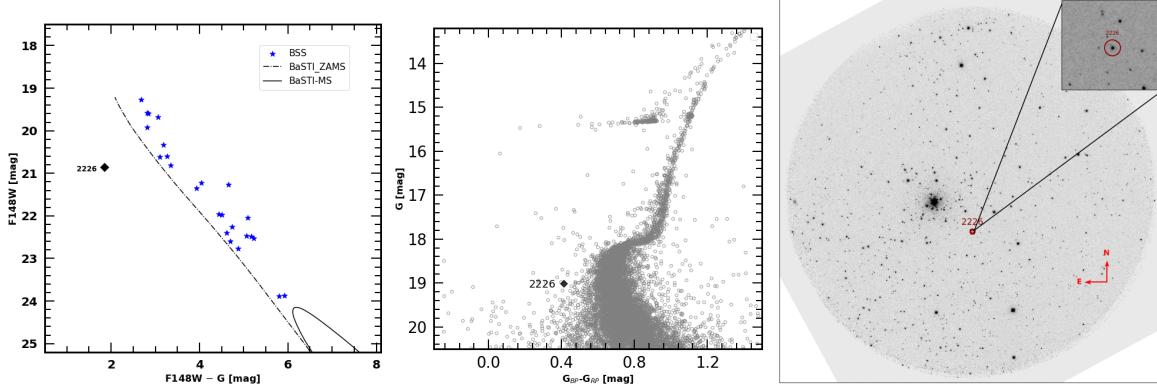


Figure 1: Left panel: UV-optical CMD (F148W vs F148W – G) of the BSSs for the cluster NGC 362. Blue symbols represent the BSSs. The probable Blue straggler candidate, bluer than the ZAMS, is displayed with a black diamond symbol. Middle panel: The optical CMD (G vs $G_{BP} - G_{RP}$) of the cluster NGC 362. Right panel: Spatial locations of an FUV bright BSS candidate with a red circle in the F148W image of NGC 362. The field of view of the image is $\sim 28' \times 28'$. The zoomed region around the target star is shown in the top right corner. North is up and east is on the left.

and Main Sequence curves derived from BaSTI¹. We have found an FUV bright star below the ZAMS indicated by no. 2226 and shown with a black diamond. To cross-check the position of the star 2226 in the optical CMD, we created a (G, ($G_{BP} - G_{RP}$)) diagram, as shown in the middle panel of Figure 1. The diagram clearly indicates that star 2226 aligns below the BSS sequence of the cluster. In order to validate the position of the star 2226 and assess any potential contamination, we carefully inspected the observed image. The right panel of Figure 1 depicts the F148W image, where we marked the position of the star 2226 with a red square. The image reveals that this star is well-resolved and exhibits no signs of contamination.

As BSSs are often formed through interactions between stars, it is plausible that some BSSs have a companion in the form of a binary system. This companion could exist either as the outer component of a triple system or as a remnant of a donor star after Mass Transfer (MT) has occurred. Analyzing the SEDs of these systems allows us to determine the characteristics of their multiple components. The successfully detected companions known as ELM WDs associated with BSSs indicate that these systems have undergone MT (Dattatrey et al., 2023).

4. SPECTRAL ENERGY DISTRIBUTION

SED modeling involves fitting theoretical models or templates to the observed data to derive the physical parameters of the object, such as its temperature, luminosity, and radius. As a virtual observatory tool, VOSA (VO SED Analyzer) (Bayo et al., 2008) is used in this work. The produced synthetic photometric data is compared with the observed data to find the best fit using the χ^2 minimization test. We used the Castelli and Kurucz (2003) model with a full range of all parameters such as the effective temperatures (T_{eff}) from 5000-50000 K, with a

¹<http://basti-iac.oa-abruzzo.inaf.it/>

metallicity of $[\text{Fe}/\text{H}] = -1$, which is close to the metallicity of the cluster, and a $\log g$ of 3-5 dex provided in VOSA for the cool component. To account for the UV excess observed in the data, we employed two-component SED. For the hotter component, we used the Koester model (Koester, 2010) with a full range of parameters such as the T_{eff} and $\log g$ range from 5000–80000 K and 6.5–9.5, respectively.

First, we fitted a SED with a single component, as depicted by the grey curve in the left panel of Figure 2. The data points used for fitting are depicted as green, cyan, and red-filled circles with error bars, whereas model data points are depicted as blue points. The residual between the fitted model and the observed fluxes, normalized by the observed flux, is displayed in the bottom panel of Figure 2 (left panel). The dashed horizontal lines at 0.3 (30%) represent the threshold. The residual plot for the star 2226 reveals that the UV residual flux is more significant than 0.3 for multiple data points. This indicates that there is an UV excess, and the SED may be fitted by a combination of hot and cool spectra. Therefore, a two-component SED is fitted, as depicted in Figure 2 (left panel). The combined spectrum is shown with a magenta line. The fitting parameters for combine spectra such as χ^2 , V_{gf} , and V_{gf_b} are 22.63, 19.0, and 4.0 respectively.

The fractional residual points for the combined SED is well fitted with 0.3 shown by blue points. The Fundamental properties of the star 2226, including the T_{eff} , $\log g$, luminosity, and radius of the cool component (2226A) are estimated to be 7250_{-125}^{+125} K, 5, $1.97_{-0.020}^{+0.181}$ L_{\odot} , and $0.89_{-0.06}^{+0.03}$ R_{\odot} , whereas for the hot component (2226B) are 15000_{-1000}^{+250} K, 9.5, $1.40_{-0.10}^{+0.09}$ L_{\odot} , and $0.17_{-0.01}^{+0.03}$ R_{\odot} .

4.1. HERTZSPRUNG-RUSSELL DIAGRAM

To estimate the age and mass of the cool component (2226A), we utilized the Hertzsprung-Russell (H-R) diagram shown in Figure 2. By comparing the position of the cool component, represented by the blue point, with theoretical isochrones retrieved from BaSTI (Pietrinferni et al., 2021), we can determine their age and mass. In the H-R diagram, we plotted the 1 Gyr isochrone using the blue line. By evaluating the position of the cool component (2226A), we estimated the age and mass of BSSc as ~ 1 Gyr and $1.77 M_{\odot}$, respectively.

For the hot components (2226B), we also determined the age and mass using the H-R diagram displayed in the right panel of Figure 2. By considering the surface temperature and luminosity derived from the SED analysis, we positioned the hot component (2226B) with cyan point. By examining the position of the hot component relative to the ELM tracks, we estimated cooling age and mass to be ~ 4 Myr and $0.19\text{-}0.20 M_{\odot}$, respectively.

5. Results and discussion

In the present study, we identified an FUV bright BSSc in the globular cluster NGC 362. We constructed SED using the VOSA tool to analyze the physical characteristics of BSSc and investigate the presence of any companion. Fitting single-component SEDs to the observed data points revealed UV excess in the BSSc, indicating the need for two-component SED fitting. By

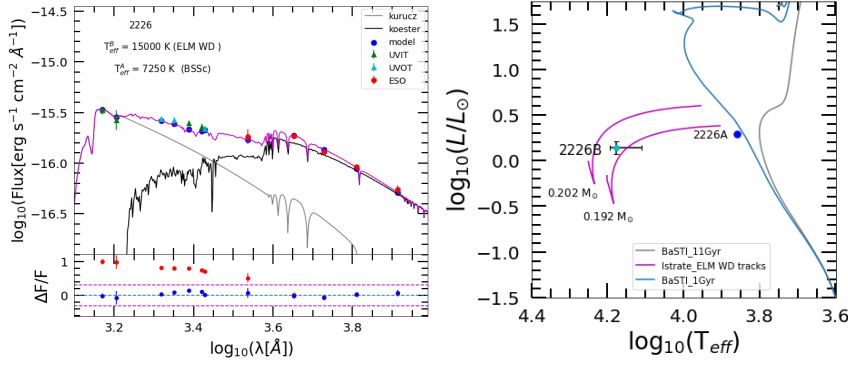


Figure 2: Left panel, the SED of bright BSS candidate star. The T_{eff} of the cool (A) and hot (B) components are displayed in SED. The observed data points are represented by green, cyan, and red points representing UVIT, UVOT, and ESO data respectively, while blue points represent the model points. Black, grey, and magenta curves represent the Koester, Kurucz, and combined spectra, respectively. $\Delta F/F$ is the fractional residual. Right Panel, the HR diagram of the cool (blue) and hot (cyan) components. The grey curve represents the BaSTI isochrones. The ELM tracks are represented by the magenta curves with masses around 0.192 and $0.202M_{\odot}$.

fitting the SED with combined spectra of cool and hot components, we achieved good fits for BSSc. This suggests that BSSc is part of the binary system. The hot component denoted as 2226B, exhibited a surface temperature of 15000 K, luminosity of $1.40 L_{\odot}$, and radii of $0.17 R_{\odot}$, while for cool component, it is 7250 K, $1.97 L_{\odot}$, and $0.89 R_{\odot}$ respectively. Based on the above parameters, we suggest that cool component may be BSSc and hot component can be ELM WD.

Based on the literature survey, the ELM WD can be found in binaries (Dattatreya et al., 2023), indicating the formation process via mass transfer (MT) processes. The presence of low-mass WDs in tight binary systems suggests that the companion star removes the progenitor's envelope, leading to the formation of low-mass WDs without igniting the helium core. In this case of BSSc, this system likely formed through MT with a ELM WD companion. The formation of this binary system may be related to the dynamical evolution of the cluster. The cooling age of the ELM WD indicates that this system has recently formed. Binary systems such as BSS+ELM WDs are uncommon in GCs. Dattatreya et al. (2023) identified 12 such systems in the GC NGC 362 for the first time. UV data are highly valuable in identifying such systems.

6. Summary and Conclusions

The UVIT, UVOT, Gaia EDR3, and the 2.2m ESO/MPI telescopes provide data of BSSc in NGC 362. We found a BSSc with an ELM WD companion. Based on their location in the HR diagram, the hot and cool components are classified as ELM WD and BSSc, respectively. The ELM WD accompanied by BSSc formed via the Case A/B mass transfer pathway.

The telescopes under BINA collaborations are extremely helpful for the type of analysis

presented here. The 3.6m optical measurements are critical for the SED study. The spectroscopic observations are quite useful for characterising the BSS in the GC's outer area.

Further Information

Author contributions

This work is part of a long-term survey program and collective efforts were made by all the co-authors with the relevant contributions.

7. ACKNOWLEDGEMENTS

I express my gratitude to the reviewer for their valuable and thoughtful comments and suggestions, which significantly enhanced the quality of this manuscript.

This publication extensively utilizes data from the Astrosat mission, conducted by the Indian Space Research Organisation (ISRO) and archived at the Indian Space Science Data Centre (ISSDC). The research also leverages VOSA, a tool developed as part of the Spanish Virtual Observatory project and supported by the Spanish Ministry of Economy and Competitiveness (MINECO) through grant AyA2017-84089.

Moreover, this study relies on the software tools TOPCAT (Taylor 2005, 2011), matplotlib (Hunter 2007), and NUMPY (van der Walt, Colbert Varoquaux 2011) for data analysis and visualization. Additionally, the NASA Astrophysics Data System (ADS NASA) plays a crucial role in supporting the research.

Conflicts of interest

The authors declare no conflict of interest.

References

- Bayo, A., Rodrigo, C., Barrado Y Navascués, D., Solano, E., Gutiérrez, R., Morales-Calderón, M. and Allard, F. (2008) VOSA: virtual observatory SED analyzer. An application to the Collinder 69 open cluster. *A&A*, 492(1), 277–287. <https://doi.org/10.1051/0004-6361:200810395>.
- Benvenuto, O. G. and De Vito, M. A. (2004) The formation of a helium white dwarf in a close binary system with diffusion. *MNRAS*, 352(1), 249–257. <https://doi.org/10.1111/j.1365-2966.2004.07918.x>.
- Brown, W. R., Kilic, M., Allende Prieto, C. and Kenyon, S. J. (2010) The ELM Survey. I. A Complete Sample of Extremely Low-mass White Dwarfs. *ApJ*, 723(2), 1072–1081. <https://doi.org/10.1088/0004-637X/723/2/1072>.

- Castelli, F. and Kurucz, R. L. (2003) New Grids of ATLAS9 Model Atmospheres. In *Modelling of Stellar Atmospheres*, edited by Piskunov, N., Weiss, W. W. and Gray, D. F., vol. 210, p. A20. <https://doi.org/10.48550/arXiv.astro-ph/0405087>.
- Dattatreya, A. K., Yadav, R. K. S., Rani, S., Subramaniam, A., Singh, G., Sahu, S. and Singh, R. S. (2023) GlobULEs. IV. UVIT/AstroSat Detection of Extremely Low Mass White Dwarf Companions to Blue Straggler Stars in NGC 362. *ApJ*, 943(2), 130. <https://doi.org/10.3847/1538-4357/acade0>.
- Harris, W. E. (2010) A New Catalog of Globular Clusters in the Milky Way. *arXiv e-prints*, arXiv:1012.3224.
- Koester, D. (2010) White dwarf spectra and atmosphere models. *MmSAI*, 81, 921–931.
- Pietrinferni, A., Hidalgo, S., Cassisi, S., Salaris, M., Savino, A., Mucciarelli, A., Verma, K., Silva Aguirre, V., Aparicio, A. and Ferguson, J. W. (2021) Updated BaSTI Stellar Evolution Models and Isochrones. II. α -enhanced Calculations. *ApJ*, 908(1), 102. <https://doi.org/10.3847/1538-4357/abd4d5>.
- Poole, T. S., Breeveld, A. A., Page, M. J., Landsman, W., Holland, S. T., Roming, P., Kuin, N. P. M., Brown, P. J., Gronwall, C., Hunsberger, S., Koch, S., Mason, K. O., Schady, P., vanden Berk, D., Blustin, A. J., Boyd, P., Broos, P., Carter, M., Chester, M. M., Cucchiara, A., Hancock, B., Huckle, H., Immler, S., Ivanushkina, M., Kennedy, T., Marshall, F., Morgan, A., Pandey, S. B., de Pasquale, M., Smith, P. J. and Still, M. (2008) Photometric calibration of the Swift ultraviolet/optical telescope. *MNRAS*, 383(2), 627–645. <https://doi.org/10.1111/j.1365-2966.2007.12563.x>.
- Sahu, S., Subramaniam, A., Singh, G., Yadav, R., Valcarce, A. R., Choudhury, S., Rani, S., Prabhu, D. S., Chung, C., Côté, P., Leigh, N., Geller, A. M., Chatterjee, S., Kameswara Rao, N., Bandyopadhyay, A., Shara, M., Dalessandro, E., Pandey, G., Postma, J. E., Hutchings, J., Simunovic, M., Stetson, P. B., Thirupathi, S., Puzia, T. and Sohn, Y.-J. (2022) Globular Cluster UVIT Legacy Survey (GlobULEs) - I. FUV-optical colour-magnitude diagrams for eight globular clusters. *MNRAS*, 514(1), 1122–1139. <https://doi.org/10.1093/mnras/stac1209>.
- Tandon, S. N., Hutchings, J. B., Ghosh, S. K., Subramaniam, A., Koshy, G., Girish, V., Kamath, P. U., Kathiravan, S., Kumar, A., Lancelot, J. P., Mahesh, P. K., Mohan, R., Murthy, J., Nagabhushana, S., Pati, A. K., Postma, J., Rao, N. K., Sankarasubramanian, K., Sreekumar, P., Sriram, S., Stalin, C. S., Sutaria, F., Sreedhar, Y. H., Barve, I. V., Mondal, C. and Sahu, S. (2017) In-orbit Performance of UVIT and First Results. *Journal of Astrophysics and Astronomy*, 38(2), 28. <https://doi.org/10.1007/s12036-017-9445-x>.
- Vasiliev, E. and Baumgardt, H. (2021) Gaia EDR3 view on galactic globular clusters. *MNRAS*, 505(4), 5978–6002. <https://doi.org/10.1093/mnras/stab1475>.